LEGIBILITY NOTICE

A major purpose of the Technical Information Center is to provide the broadest dissemination possible of information contained in DOE's Research and Development Reports to business, industry, the academic community, and federal, state and local governments.

Although a small portion of this report is not reproducible, it is being made available to expedite the availability of information on the research discussed herein.

LA-UR 90-1386

CONF-9009134--1

MAY 0 3 1990

Los Alamos National Laboratory is operated by the University of California for the United States Department of Energy under contract W-7405-ENG-36

LA-UR--90-1386

DE90 010612

TITLE Three-dimensional Forcasting Models on a Desk-Top Computer

AUTHOR(S) T. Yamada, and S. Bunker

SUBMITTED TO 3rd International Conference, ENVIRONSOFT 90, Montreal, Canada, September 11-13, 1990

DISCLAIMER

MASTER

Los Alamos Los Alamos National Laboratory
Los Alamos, New Mexico 87545

FORM NO. 836 R4
ST. NO. 2629 5/81

DISTRIBUTION OF THIS DOCUMENT IS UNLIMITED

Three-dimensional Forecasting Models on a Desk-Top Computer

T. Yamada and S. Bunker *Los Alamos National Laboratory, Los Alamos, New Mexico, U.S. A.*

INTRODUCTION

Recent advances in the desk-top computer capabilities, particularly those of an engineering workstation, are truly astonishing. A high performance workstation reportedly exceeded a supercomputer in certain scaler operations. Affordability and portability of a desk-top computer opened doors to many applications which were previously considered impossible.

The purpose of the present study is to demonstrate the feasibility of using an engineering workstation to operate a three-dimensional mesoscale modeling system to describe the transport and dispersion of atmospheric pollutants over complex terrain surrounding Vandenberg Air Force Base (VAFB), Vandenberg, California.

Our modeling system is composed of two numerical codes, HOTMAC (Higher Order Turbulence Model for Atmospheric Circulations) and RAPTAD (RAndom Puff Transport And Diffusion). HOTMAC is a mesoscale forecast code that is able to model three-dimensional distributions of wind speed, wind direction, turbulence, temperature, and water vapor. RAPTAD is a Lagrangian puff code based on the Monte Carlo statistical diffusion process. RAPTAD can be used under extreme conditions where a conventional Gaussian plume model may fail.

MODEL EQUATIONS

HOTMAC

The basic equations for mean wind, temperature, mixing ratio of water vapor, and turbulence are similar to those used by Yamada and Bunker.[1].

A terrain-following vertical coordinate system is used in order to increase the accuracy in the treatment of surface boundary condition:

$$z^* = H \frac{z - z_g}{H - z_g} \quad , \tag{1}$$

where z^* and z are transformed and Cartesian vertical coordinates, respectively; z_g is ground elevation; H is the material surface top of the model in the z^* coordinate and H is the corresponding height in the z-coordinate.

The governing equations, following the coordinate transformation, are:[1]

$$\frac{DU}{Dt} = f(V - V_g) + g\frac{\overline{H} - z^*}{\overline{H}}\left(1 - \frac{\langle\Theta_v\rangle}{\Theta_v}\right)\frac{\partial z_g}{\partial x} + \frac{\partial}{\partial x}\left(K_x\frac{\partial U}{\partial x}\right) + \frac{\partial}{\partial y}\left(K_{xy}\frac{\partial U}{\partial y}\right) + \frac{\overline{H}}{H - z_g}\frac{\partial}{\partial z^*}(-\overline{uw}) \quad , \tag{2}$$

$$\frac{DV}{Dt} = -f(U - U_g) + g\frac{\overline{H} - z^*}{\overline{H}}\left(1 - \frac{\langle\Theta_v\rangle}{\Theta_v}\right)\frac{\partial z_g}{\partial y} + \frac{\partial}{\partial x}\left(K_{xy}\frac{\partial V}{\partial x}\right) + \frac{\partial}{\partial y}\left(K_y\frac{\partial V}{\partial y}\right) + \frac{\overline{H}}{H - z_g}\frac{\partial}{\partial z^*}(-\overline{vw}) \quad , \tag{3}$$

$$\frac{\partial U}{\partial x} + \frac{\partial V}{\partial y} + \frac{\partial W^*}{\partial z^*} - \frac{1}{H - z_g}\left(U\frac{\partial z_g}{\partial x} + V\frac{\partial z_g}{\partial y}\right) = 0 \quad , \tag{4}$$

where

$$W^* \equiv \frac{\overline{H}}{H - z_g}W + \frac{z^* - \overline{H}}{H - z_g}\left(U\frac{\partial z_g}{\partial x} + V\frac{\partial z_g}{\partial y}\right) \quad , \tag{5}$$

and

$$\frac{D(\ )}{Dt} \equiv \frac{\partial(\ )}{\partial t} + U\frac{\partial(\ )}{\partial t} + V\frac{\partial(\ )}{\partial y} + W^*\frac{\partial(\ )}{\partial z^*} \quad . \tag{6}$$

In the above expressions, $\langle\ \rangle$ indicates an average over a horizontal surface. The second terms on the right-hand side of Equations (2) and (3) indicate the effects of ground slope. For simplicity, H is specified as

$$H = \overline{H} + z_{gmax}, \tag{7}$$

where $\overline{H} = 5000$ m and $z_{gmax} = 565.7$ m are used in this study. Expressions of the horizontal eddy viscosity coefficients, K_x, K_y, and K_{xy} are given in Yamada.[2]

The geostrophic winds U_g and V_g are computed from Yamada;[3]

$$fU_g \equiv fU_g(\overline{H})\frac{\langle\Theta_v\rangle}{\langle\Theta_v(\overline{H})\rangle} + g\frac{H - z_g}{\overline{H}}\int_{z_\cdot}^{\overline{H}} \frac{1}{\langle\Theta_v\rangle} \times \frac{\partial}{\partial y}\Delta\Theta_v dz' - \frac{g}{\overline{H}}\frac{\partial z_g}{\partial y}\int_{z_\cdot}^{\overline{H}} \frac{\Delta\Theta}{\langle\Theta_v\rangle_v} dz' \tag{8}$$

and

$$fV_g \equiv fV_g(\overline{H})\frac{\langle\Theta_v\rangle}{\langle\Theta_v(\overline{H})\rangle} - g\frac{H - z_g}{\overline{H}}\int_{z_\cdot}^{\overline{H}} \frac{1}{<\Theta_v>}\frac{\partial\Delta\Theta_v}{\partial x}dz' + \frac{g}{\overline{H}}\frac{\partial z_g}{\partial x}\int_{z_\cdot}^{\overline{H}} \frac{\Delta\Theta_v}{\langle\Theta_v\rangle}dz' \quad , \tag{9}$$

where $\Delta\Theta_v \equiv \Theta_v - \langle\Theta_v\rangle$, and the abbreviated symbols $U_g(\overline{H}) \equiv U_g(x, y, \overline{H}, t)$; $V_g(\overline{H}) \equiv V_g(x, y, \overline{H}, t)$ etc. are used. The derivations of Equations (2)-(5), (8), and (9) are given in the Appendix of Yamada.[3] A turbulence kinetic energy equation is given by

$$\frac{D}{Dt}\left(\frac{q^2}{2}\right) = \frac{\partial}{\partial x}\left[K_x\frac{\partial}{\partial x}\left(\frac{q^2}{2}\right)\right] + \frac{\partial}{\partial y}\left[K_y\frac{\partial}{\partial y}\left(\frac{q^2}{2}\right)\right] + \left(\frac{\overline{H}}{H - z_g}\right)^2\frac{\partial}{\partial z_\cdot}\left[qlS_q\frac{\partial}{\partial z_\cdot}\left(\frac{q^2}{2}\right)\right] - \frac{\overline{H}}{H - z_g} \times \left(\overline{uw}\frac{\partial U}{\partial z_\cdot} + \overline{vw}\frac{\partial V}{\partial z_\cdot}\right) + \beta g\overline{w\theta_v} - \frac{q^3}{B_1\ell} \tag{10}$$

and a turbulence length scale ℓ is obtained from

$$\frac{D}{Dt}(q^2\ell) = \frac{\partial}{\partial x}\left[K_x\frac{\partial}{\partial x}(q^2\ell)\right] + \frac{\partial}{\partial y}\left[K_y\frac{\partial}{\partial y}(q^2\ell)\right] + \left(\frac{\overline{H}}{H - z_g}\right)^2\frac{\partial}{\partial z_\cdot}\left[qlS_\ell\frac{\partial}{\partial z_\cdot}(q^2\ell)\right]$$

$$+ \ell F_1 \left[\frac{\overline{H}}{H - z_g} \left(- \overline{uw} \frac{\partial U}{\partial z*} - \overline{vw} \frac{\partial V}{\partial z} \right) + \beta g \overline{w\theta_v} \right]$$

$$- \frac{q^3}{B_1} \left[1 + F_2 \left(\frac{1}{kz} \right)^2 \right] \qquad (11)$$

where $\overline{q^2} = \overline{u^2} + \overline{v^2} + \overline{w^2}$ is twice the turbulence kinetic energy; $\overline{w\theta_v}$, turbulence heat flux; θ_v, the fluctuation part of virtual potential temperature, and $(F_1, F_2, S_q, S_\ell$, and $B_1) = (1.8, 1.33, 0.2, 0.2$, and $16.6)$, empirical constants determined from laboratory experiments (Mellor and Yamada[4]).

The internal heat energy equation is written in terms of $\Delta\Theta_v$ as discussed in Yamada and Bunker.[5] We obtain a prognostic equation for $\Delta\Theta_v$ as

$$\frac{D\Delta\Theta_v}{Dt} = \frac{\partial}{\partial x} \left(K_x \frac{\partial \Delta\Theta_v}{\partial x} \right) + \frac{\partial}{\partial y} \left(K_y \frac{\partial \Delta\Theta_v}{\partial y} \right)$$

$$+ \frac{\overline{H}}{H - z_g} \left[\frac{\partial}{\partial z^*} (-\overline{w\theta_v}) + \frac{1}{\rho C_p} \frac{\partial R_N}{\partial z^*} - W \frac{\partial \Theta_v}{\partial z^*} \right] , \qquad (12)$$

where $\partial < \Theta_v > /\partial x = \partial < \Theta_v > /\partial y = 0$ are used.

The longwave radiation flux $R_N/\rho C_p$ is computed according to Sasamori.[6] A conservation equation for mixing ratio of water vapor is given by

$$\frac{\partial Q_v}{\partial t} = \frac{\partial}{\partial x} \left[K_x \frac{\partial Q_v}{\partial x} \right] + \frac{\partial}{\partial y} \left[K_y \frac{\partial Q_v}{\partial y} \right]$$

$$+ \frac{\overline{H}}{H - z_g} \frac{\partial}{\partial z^*} (-\overline{wq_v}) , \qquad (13)$$

The turbulent fluxes in Equations (2), (3), (10), (11), (12), and (13) are obtained from simplified second-moment turbulence-closure equations (Yamada[7]):

$$(\overline{uw}, \overline{vw}) = -lq\tilde{S}_M \left(\frac{\partial U}{\partial z}, \frac{\partial V}{\partial z} \right) \qquad (14a, b)$$

$$(\overline{w\theta_v}, \overline{wq_v}) = -alq\tilde{S}_M \left(\frac{\partial \Theta_v}{\partial z}, \frac{\partial Q_v}{\partial z} \right) , \qquad (15a, b)$$

where $\widetilde{S}_M$ and α are functions of the flux Richardson number, and $\alpha(\equiv K_H/K_M$ where K_H is an eddy diffusivity coefficient and K_M is an eddy viscosity coefficient) is the reciprocal of the turbulent Prandtl number. The expressions for $\widetilde{S}_M$ and α are obtained from the level 2 model (production = dissipation) of Mellor and Yamada[8] where temporal and spatial derivatives in Eq. (9) are neglected. The readers are referred to Yamada[9] for further discussions of the level 2 model equations. The final expressions for $\widetilde{S}_M$ and α are given in (Yamada[7]) and are not repeated here.

RAPTAD

A brief description of RAPTAD (Yamada and Bunker[1]) is given herein. Locations of the center of each puff are computed from

$$x_i(t + \Delta t) = x_i(t) + U_{pi}\Delta t \tag{16}$$

where

$$U_{pi} = U_i + u_i \quad , \tag{17}$$

$$u_i(t + \Delta t) = au_i(t) + b\sigma u_i\zeta \tag{18}$$

$$a = \exp\left(-\Delta t/t_{Lx_i}\right) \quad , \tag{19}$$

and

$$b = (1 - a^2)^{1/2} \quad . \tag{20}$$

In the above expressions, U_{pi} is the particle velocity in the x_i direction; U_i, mean velocity; u_i, turbulence velocity; ζ, a random number from a Gaussian distribution with zero mean and unit variance, t_{Lx_i}, the Lagrangian integral time for the velocity u_i; and σ_{ui}, standard deviation of velocity fluctuation, u_i.

The Lagrangian time scales, $t_{Lx} = t_{Ly} = 10^4 s$ (Gifford[10]) and $t_{Lz} = 20s$, (Yamada and Bunker[1]) are used in this study.

Concentration χ at (X, Y, Z) is estimated by using the following expression:

$$\chi(X, Y, Z) = \frac{Q\Delta t}{(2\pi)^{3/2}} \sum_{k=1}^{N} \frac{1}{\sigma_{xk}\sigma_{yk}\sigma_{zk}} \exp\left(-\frac{1}{2}\frac{(x_k - X)^2}{\sigma_{xk}^2}\right)$$

$$\times \exp\left(-\frac{1}{2}\frac{(y_k - Y)^2}{\sigma_{yk}^2}\right)\left\{\exp\left(-\frac{1}{2}\frac{(z_k - Z)^2}{\sigma_{zk}^2}\right)\right.$$
$$\left. + \exp\left(-\frac{1}{2}\frac{(z_k + Z - 2z_g)^2}{\sigma_{zk}^2}\right)\right\} \quad , \tag{21}$$

where (x_k, y_k, z_k) is the location of kth particle; σ_{xk}, σ_{yk}, and σ_{zk} are standard deviations of a Gaussian distribution; and z_g is the ground elevation. The variances are estimated based on Taylor's[11] homogeneous diffusion theory. For example, σ_y is obtained from

$$\sigma_y^2 = 2\sigma_v^2 \int_0^t \int_0^\zeta K(\zeta) d\zeta dt$$
$$= 2\sigma_v^2 t_{Ly}\left(t + t_{Ly} \exp\left(-\frac{t}{t_{Ly}}\right) - t_{Ly}\right) \quad , \tag{22}$$

where a correlation function $R(\zeta) = \exp(-\zeta/t_{Ly})$ is used.

In a similar fashion, σ_x and σ_z are determined. The standard deviations σ_u, σ_v and σ_w at each particle location are obtained by interpolating grid values of a computation grid volume in which a particle is located.

SIMULATIONS AND DISCUSSIONS

The Mountain Iron (MI) diffusion experiments (Hinds and Nickola[12]) were conducted at Vandenberg Air Force Base during 1965 and 1966 to establish quantitative diffusion predictions for use as range safety tools in the "South Vandenberg" (SV) ballistic and space vehicle operations.

The experimental site, SV, is located along the California coast approximately 160 km west-northwest of Los Angeles. The coastline is oriented in approximately a north-south direction along the western side of SV, but changes abruptly at Point Arguello to a east-west direction. The coastline gradually changes to a north-south direction down to Point Conception and then changes again to a east-west direction. Santa Ynez Mountains form a east-west barrier along the coastline far south of SV.

The purpose of the present study is to demonstrate the feasibility of using an engineering workstation to operate three-dimensional models under realistic boundary conditions: land-sea contrast and complex topography. Thus, only qualitative discussions are given here, and more detailed study on model-observation comparisons is found in Yamada and Bunker.[13]

We selected the MI87 case which was characterized (Hunter[14]) as "Weak ambient and sea-breeze flow, with little distinction between wind vectors, but sharp cooling with fog rolling in."

Initial potential temperature profile was determined from the upper air soundings at 1300 lst. The potential temperature lapse rate was approximately 0.04°C/m from the sea surface to 460 m msl and 0.044°C/m above 460 m msl. Prevailing wind speed (2 m/s) and direction (225°C) were determined by examining five upper air soundings at 1300 lst.

The computational domain is 40 x 48 km^2 with a horizontal grid spacing of 1 km. Integration started at 0500 lst, June 13, 1966 and continued for over 48 hours. The model plume was released continuously for 24 hrs starting at 2300 lst to examine the diurnal variation of the plume transport and diffusion processes.

Figure 1 shows the modeled horizontal wind vectors at 14 m above the ground at 0700 lst, June 14. Although the upper air wind direction was 225°C (southwesterly) downslope flows and land breeze developed in the surface layer due to cooling at the ground. The sunrise on June 14, 1966 was shortly before 0500 lst.

As the sun warms the ground, the air temperature in the surface layer first increases by convection. The air temperature over a sloped surface becomes higher than the temperature at the same elevation but away from the ground. The temperature difference results in a horizontal pressure gradient: a low pressure is normally located at a high elevation point. This pressure force produces upslope flows and sea-breezes that converge into ridges (Fig. 2).

The ground starts cooling shortly before sunset (around 2000 lst) and the air temperature close to the ground over a sloped surface is now lower than the air temperature at the same elevation but away from the surface. Thus, the direction of pressure gradient in the nighttime reverses from the daytime counterpart. However, the magnitude of the nighttime pressure force is normally much smaller than the daytime value, particularly in the summer season, for the following reasons.

First, turbulence intensity in the surface layer during the nocturnal period is extremely small, comparing with the daytime value. Therefore, only the air relatively close to the ground is cooled by turbulent mixing. The depth of the noctural stable boundary layer is on the order of 100 m which is much smaller than the daytime convective boundary layer height of at least several hundred meters.

Second, the solar energy that reaches the ground in Summer is far larger than the net longwave radiation loss during the nighttime. In other words,

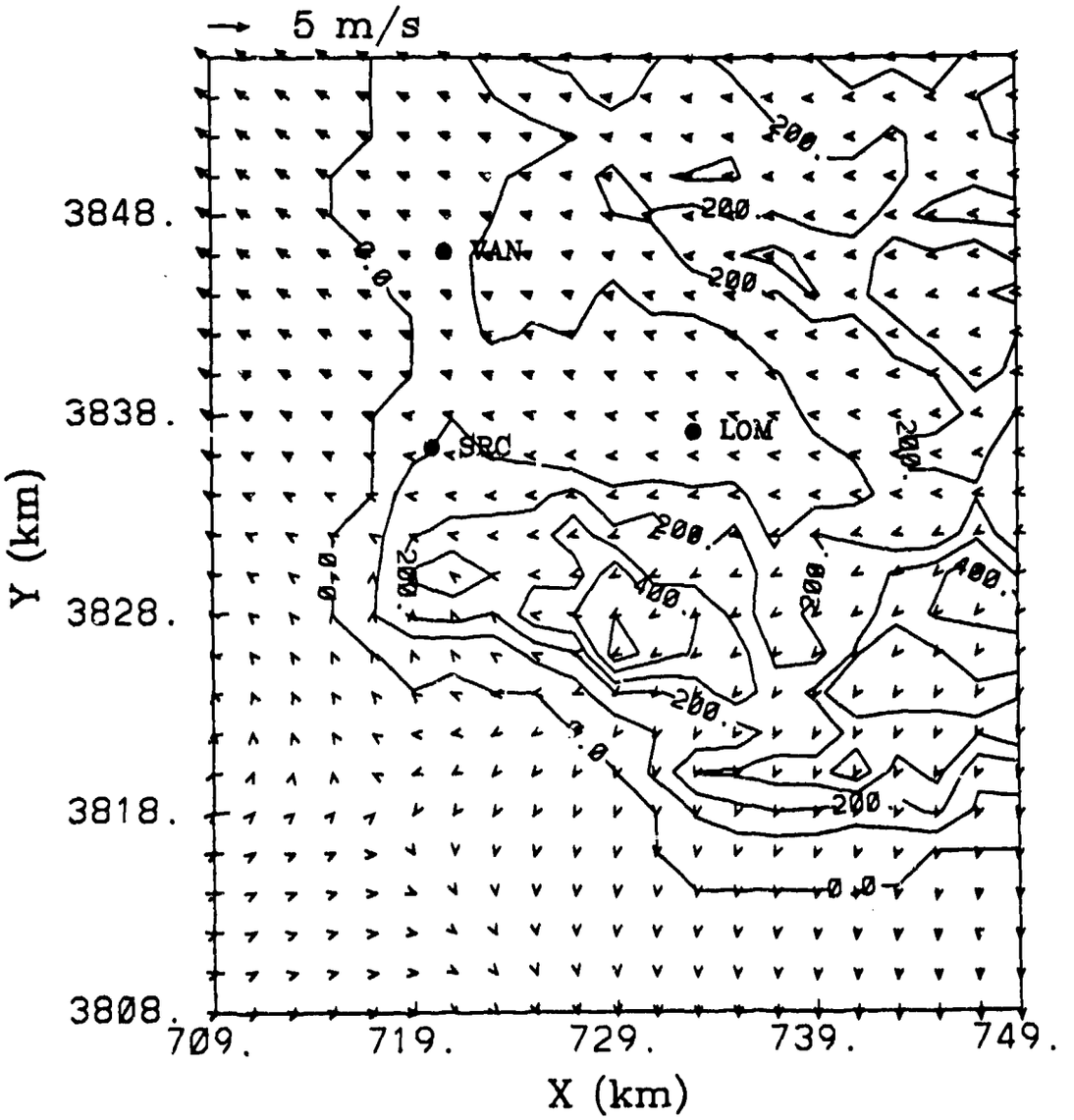

Figure 1. Modeled horizontal wind vectors at 14 m above the ground at 0700 lst, June 14, 1966. Terrain is contoured by solid lines with an increment of 100 m.

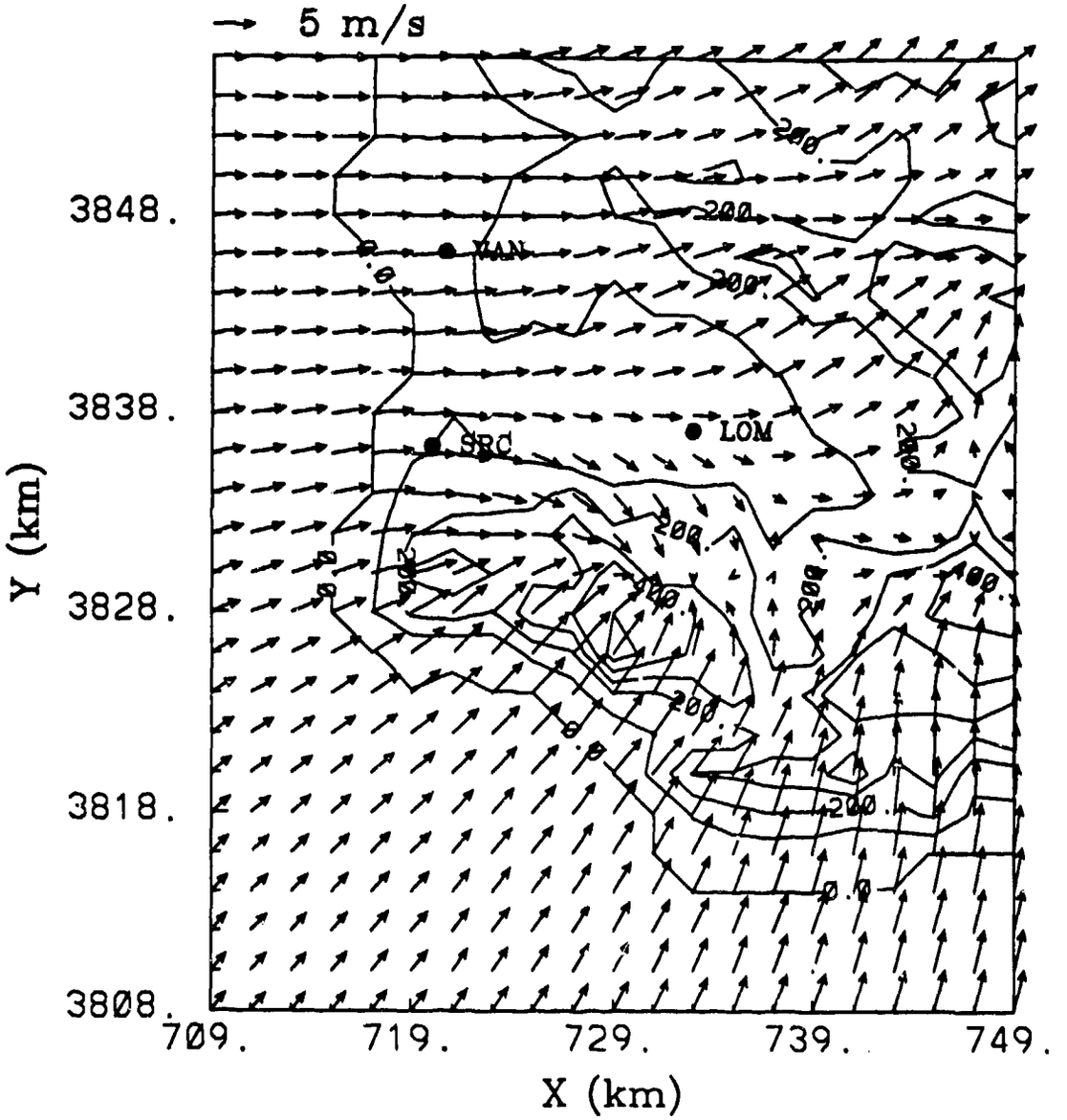

Figure 2. Modeled horizontal wind vectors at 14 m above the ground at 1400 lst, June 14, 1966. Terrain is contoured by solid lines with an increment of 100 m.

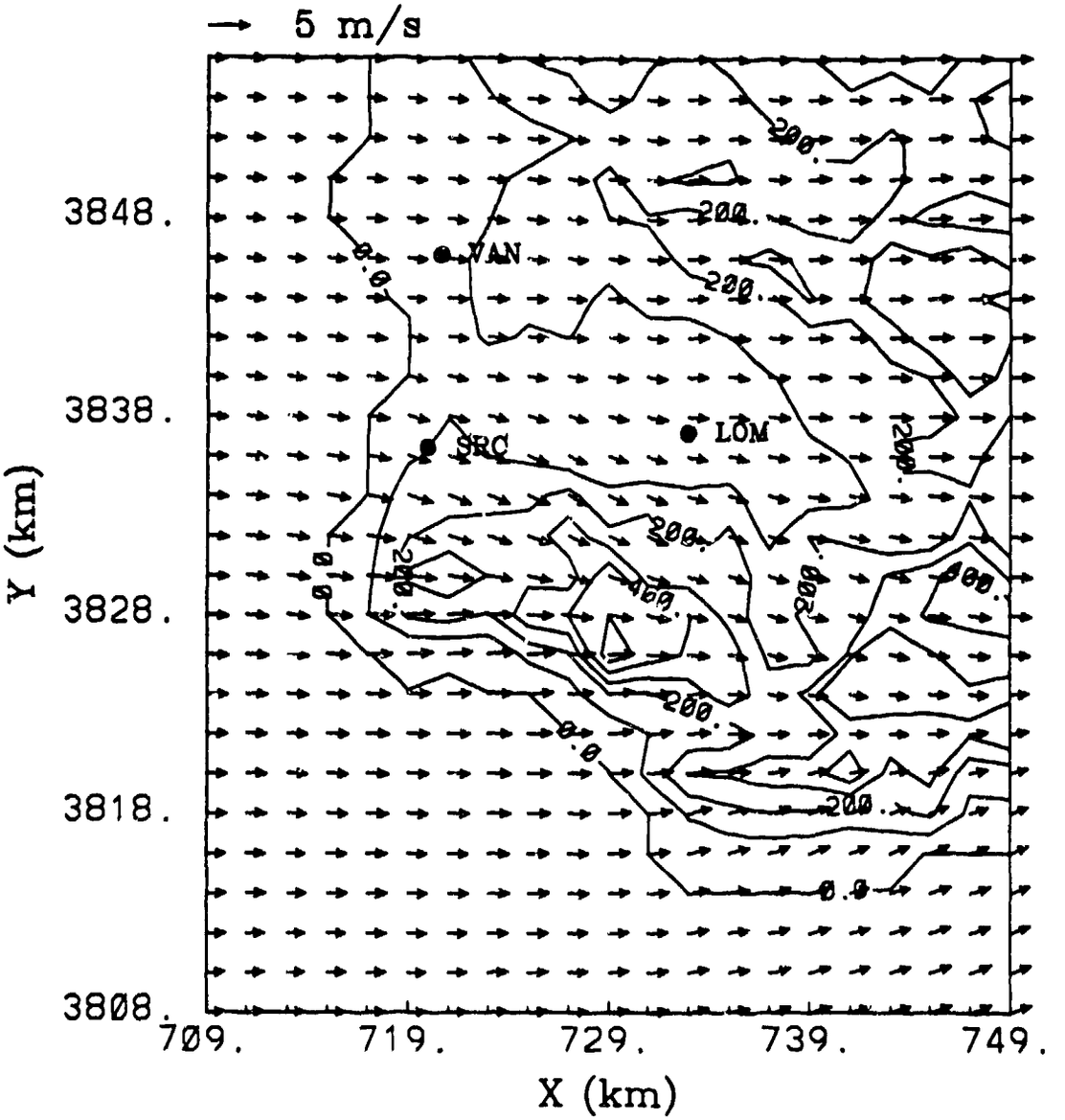

Figure 3. Modeled horizontal wind vectors at 14 m above the ground at 2300 lst, June 14, 1966. Terrain is contoured by solid lines with an increment of 100 m.

much more heat energy is input to the atmosphere during the day than the extraction of the heat energy from the atmosphere during the night.

The combination of the deeper boundary layer depth and greater heat energy available to heat the atmosphere during the daytime produced much larger pressure gradients than the nighttime counterpart. This is the reason why the modeled wind directions (Fig. 3) were not downslope although the upslope flow components encountered during the daytime (Fig. 2) almost completely diminished. The modeled wind direction later became downslope but the magnitude was very small.

ACKNOWLEDGEMENTS

The authors are grateful to Dr. J. T. Lee for reviewing, and K. Coen for typing the manuscript. The work was supported by the U. S. Air Force Engineering Service Center, Tyndall Air Force Base and U. S. Air Force Technical Application Center, Patrick Air Force Base. It was performed under the auspices of the U. S. Department of Energy at Los Alamos National Laboratory.

REFERENCES

1. Yamada T., and Bunker S. Development of a Nested Grid, Second Moment Turbulence Closure Model and Applications to the 1982 ASCOT Brush Creek Data Simulation, *J. Appl. Meteor.*,, Vol. 27,pp. 562-578, 1988.

2. Yamada, T. A Three-Dimensional, Second-Order Closure Numerical Model of Mesoscale Circulations in the Lower Atmosphere, Argonne National Laboratory, ANL/RER-78-1, 67 pp. Available from National Technical Information Service, U. S. Department of Commerce, 5285 Port Royal Road, Springfield, VA 22161, 1978.

3. Yamada, T., A Numerical Simulation of Nocturnal Drainage Flow, *J. Meteor. Soc., Japan* Vol. 59, pp. 108-122, 1981.

4. Mellor, G. I., and Yamada, T., Development of a Turbulence Closure Model for Geophysical Fluid Problems, it Rev. Geophys. Space Phys., Vol. 20, pp. 851-875, 1982.

5. Yamada, T., and Bunker, S., A Numerical Model Study of Nocturnal Drainage Flows with Strong Wind and Temperature Gradients, *J. Appl. Meteor.* Vol. 28, pp. 545-554, 1989.

6. Sasamori, T. The Radiative Cooling Calculation for Application to General Circulation Experiments, *J. Appl. Meteor.*, Vol. 7, pp. 721-729, 1968.

7. Yamada, T., Simulations of Nocturnal Drainage Flows by a $q^2\ell$ Tur-Closure Model *J. Atmos., Sci.*, Vol. 40, pp. 91-106, 1983.

8. Mellor, G. I., and Yamada, T. A Hierarchy of Turbulence-Closure Models for Planetary Boundary Layer, *J. Atmos., Sci.*, Vol. 31, pp. 1791-1806, 1974.

9. Yamada, T., The Critical Richardson Number and the Ratio of the Eddy Transport Coefficients Obtained from a Turbulence Closure Model, *J. Atmos., Sci.* Vol. 32, pp. 926-933, 1975.

10. Gifford, F. A., Horizontal Diffusion in the Atmosphere: A Lagrangian-dynamic Theory, *Atmos. Environ.* Vol. 16, pp. 505-512, 1982).

11. Taylor, G. I., Diffusion by Continuous Movements, Proceedings of the London Mathematical Society, Ser. 2 Vol. 20, pp. 196-211, 1921.

12. Hinds, W. T., and Nickola, P. W., The Mountain Iron Diffusion Program: Phase 1 South Vandenberg: Volume 1, AEC Research and Development Report, BNWC-ST2, Vol. 1, Pacific Northwest Laboratory, Batelle Memorial Institute, Richland, Washington.

13. Yamada, T. and Bunker, S., Numerical Simulations of the Mountain Iron Tracer Data, 1990 EPA, AWMA International Symposium on Measurement of Toxic and Related Air Pollutants, Raleigh, N. C., April 30-May 4, 1990.

14. Hunter, S. M., Winds on Critical Streamline Surfaces (WOCSS) Model - An Evaluation Using Vandenberg AFB Terrain and Meteorological Data, Riso National Laboratory.